Critical chloride concentrations in reinforced concrete specimens with ordinary Portland and blast furnace slag cement

J. Pacheco, R.B. Polder

Delft University of Technology, Delft, the Netherlands
TNO, Structural Reliability, Delft, the Netherlands

Chloride induced reinforcement corrosion is the predominant degradation mechanism affecting reinforced concrete structures. Chlorides (Cl⁻) contained in sea water or de-icing salts penetrate through concrete pores by diffusion and/or convection. Reinforcement corrosion initiates when the Cl concentration at the reinforcing steel surface equals or exceeds a specific concentration. This concentration is known as the critical chloride content (C_{crit}). This study presents an experimental method proposed by the RILEM Committee 235-CTC "corrosion initiating chloride threshold concentrations". Two series of reinforced concrete specimens were fabricated: one with ordinary Portland cement (CEM I) and another with ground granulated blast furnace slag –GGBS- (CEM III/B) cement, both commercially available in The Netherlands. Subsequently, the specimens were partially submerged in a chloride-rich solution (3.3 wt. % NaCl) for 6 months. During this period, continuous monitoring of the open-circuit potential (OCP) of the steel reinforcement was used to determine the initiation of reinforcement corrosion. The concentration of Cl could be determined by acid digestion and subsequent titration of powder samples collected from individual layers in the concrete cover. Results show that after the exposure period, the C_{crit} could be determined in PC specimens whereas in GGBS concrete specimens the higher resistance to chloride ingress prevented from obtaining corrosion initiation.

Key words: Critical chloride content, concrete, durability

1   Introduction

Chloride induced reinforcement corrosion is the main cause of degradation in concrete structures. Concrete alkalinity (pH > 13) protects embedded steel reinforcement due to the formation of a thermodynamically stable oxide film that forms at the steel surface, the passive film [Page 1982]. Concrete structures are often exposed to chloride-contaminated environments, causing chloride ions (Cl⁻) to penetrate through the concrete cover. The transport of Cl⁻ in (non-cracked) concrete is commonly described by Fick's second law [Collepardi *et al.,* 1972] :

$$C(x,t) = (C_s - C_i)\,\mathrm{erfc}\,\frac{x}{\sqrt{4Dt}} \tag{1}$$

with $C(x,t)$ is the chloride content (all chloride contents are expressed in wt. % of binder) at depth x at time t , C_s the surface chloride content, C_i the initial chloride content, erfc is the complementary Gaussian error function and D is the species apparent diffusion coefficient, i.e. of chlorides. Figure 1 shows the variation of the concentration of chlorides at different depths for a *constant* diffusion coefficient (D_c) over time.

Reinforcement corrosion initiates when the concentration of chlorides at the steel surface equals or exceeds a certain concentration known as the critical chloride content (C_{crit}).
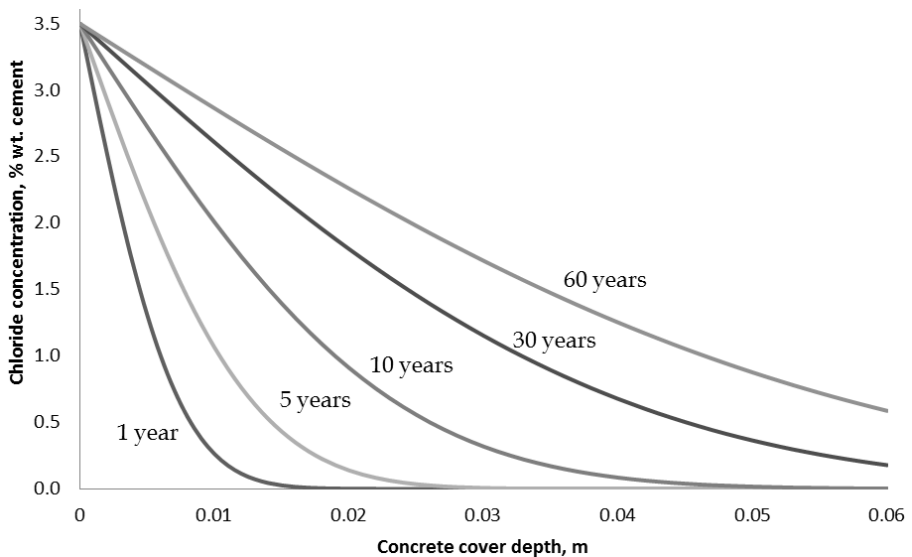

Figure 1. Chloride ingress in sound concrete

Once C_{crit} has been reached, local dissolution of the passive layer is followed by the nucleation of corrosion pits which eventually may grow. Evidence of high variability of reported C_{crit} values in the literature [Angst *et al.*, 2009] suggest that the influence of numerous parameters on C_{crit} in laboratory conditions stems from the complexity in accurate determination of this parameter and other deviations such as differences in testing conditions, quantification techniques, materials, etc.

1.1 C_{crit} in scientific research

Experimentally, C_{crit} has been studied by many researchers. Breit [Breit, 1998] studied mortar where he found a distribution in C_{crit} values with an average of 0.5 wt. % of binder and a standard deviation of 0.2%. However, the type of distribution was undefined with normal, lognormal and beta as the most probable types of distribution. Also in mortar, Alonso [Alonso *et al.*, 2000] found that the corrosion initiating Cl^-/OH^- concentrations ratio had a mean value of 0.6 in solutions simulating concrete pore solution.

The dependency of C_{crit} on electrochemical potentials was studied by Alonso [Alonso *et al.*, 2002]. The relationship between potential and corrosion initiating chloride content was found to be exponential with chloride thresholds in the range of 1.24 ± 3.08 wt. % and 0.39 ± 1.16 wt. %, for total and free chlorides, respectively. Differences between binder types were not noticed in the regions of potential values between +0.25 V_{SCE} and -0.25 V_{SCE} , characteristic of passive state. When potentials were more cathodic than -0.2 V_{SCE}, the values of free chloride threshold were increased from 1 to 4 wt. % of cement; whilst for total chloride content it varied from 1 to 8 wt. % of cement.

One of the main characteristics of chloride penetration is its inherent variability, as shown in a recent study by Angst and Polder [Angst & Polder, 2014]. Highly localised chloride content measurements were performed with ion selective electrodes (ISE). The electrodes were positioned at different locations in reinforced concrete specimens subjected to wet-dry cycles. The measured chloride concentration of parallel ISE electrodes had variations of up to 60%. These results were compared to field investigations of chloride content measurements performed on drilled cores. In both cases, the values of chloride content on both macroscopic and microscopic scales showed that the variation in chloride content is independent of the measurement technique or scale of sampling. The main cause was attributed to the influence of impermeable aggregate particles, specimen dimensions and

the maximum aggregate size ($d_{\max}$)-to-cover depth ratio. The implications from these observations are that a large variation of chloride content values at the level of the reinforcement and the bulk matrix can be expected.

1.2 C_{crit} *and service life of concrete structures*

Many Service life models based on reinforcement corrosion define the initiation of reinforcement corrosion as the end of the initiation period (t_i) [Tuutti 1982] (Figure 2). Predictions of t_i can be performed according to several service life design models, based on Fick's second law. More recently developed approaches include a semi- or fully probabilistic format [Duracrete 2000, *fib* 2006]. Irrespective of the model, the key parameter determining the duration of t_i is C_{crit}. The implications related to inaccurate determination of C_{crit} on predictions of the service life of concrete structures can lead to significant over or under estimations of t_i. Frederiksen [Frederiksen, 2009] published an overview of the existing values of C_{crit} in literature for service life design and modelling. He found that in service life modelling (design) in practice, not much effort was put in obtaining a value for C_{crit} that could be justified to be representative for the structure, the environment or the concrete composition to be used. Often values 0.05 wt. % of concrete or 0.4-0.6 wt. % of cement are used as the values to be used as an acceptable level. Accurate values for C_{crit} are crucial for service life predictions with a high degree of reliability.

Aside from the influence of parameters of cementitious or electrochemical nature, one of the crucial causes of the high variability of C_{crit} values reported in the literature is the
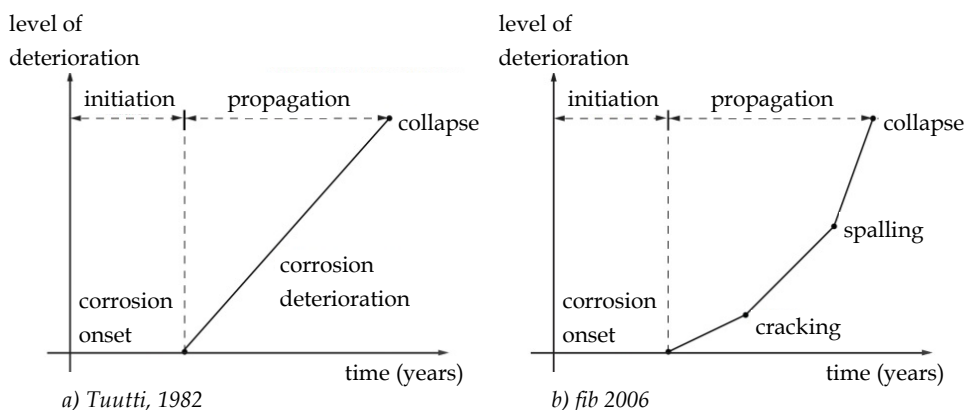

a) Tuutti, 1982   *b) fib 2006*

Figure 2. Service life modelling of concrete structures

absence of a standard test method in laboratory conditions. RILEM Technical Committee 235-CTC "corrosion initiating chloride threshold concentrations" worked on the development of a test method for determining C_{crit} in laboratory conditions [RILEM TC 235-CTC]. This paper presents the results obtained when studying C_{crit} in reinforced concrete specimens fabricated with local (Dutch) ordinary Portland cement (CEM I) and ground granulated blast furnace slag (CEM III/B) cement following an early version of a setup proposed by the RILEM Committee. Changes that were later made most likely would not have influenced the results presented herein.

2 Materials and methods

2.1 Cement

Two series of specimens were prepared, one with ordinary Portland cement (CEM I 52.5 R) and another ground granulated blast furnace slag cement (CEM III/B 42.5 N LH) both commercially available in The Netherlands. The chemical composition of both cement types is shown in Table 1; the slag cement contains about 70% slag. For the remaining of this article, the series with Portland cement will be noted as PC whereas the specimens with blast furnace slag cement with BFS.

Table 1. Chemical composition of CEM I and CEM III/B cements, wt. % of oxides

Cement	CaO	SiO_2	Al_2O_3	Fe_2O_3	K_2O	Na_2O	SO_3
CEM I 52.5R	63.98	19.76	4.93	3.16	0.54	0.27	3.17
CEM III/B 42.5N LH	46.08	29.12	10.5	1.32	0.49	0.33	3.01
	MgO	TiO_2	Mn_3O_4	P_2O_5	Cl	LOI	
CEM I 52.5R	1.92	0.28	0.11	0.77	0.04	1.65	
CEM III/B 42.5N LH	7.47	0.81	0.24	0.21	0.07	1.57	

2.2 Steel

Reinforcing steel bars with a strength class of fy ≥ 500 MPa, (EN 10080-D-Class B, Class B according to EN 1992-1-1:2005) were employed. The ribbed bars were 12 mm in diameter and 120 mm in length. A single bar was placed at the geometrical centre of the moulds with 10 mm protruding from the concrete cast surface (see below). The surface condition of the bars was as-received. Light brown rust covered portions of their surfaces.

2.3 Concrete composition

The concrete mixtures employed for the fabrication of the specimens are shown in Table 2. The water-to-binder ratio was set to 0.45. The cement content was 368 kg/m³. A high range superplastizicer (CUGLA Cretoplast SL-01 35% SPL, according to NEN - EN 934-2) was added in a dosage of 1.4% by dry mass of cement for workability purposes. The measured slump [ASTM C143/C143M] and the air content [ASTM C231/C231M] of both concrete mixes are presented in Table 2.

Table 2. Concrete mixtures composition

Material	CEM I 52.5 R	CEM III/B 42.5N LH
Cement content [kg/m³]	368	368
Water-cement-ratio [-]	0.45	0.45
Fine aggregate (< 4 mm) [kg/m³]	842	842
Coarse aggregate (4 to 16 mm) [kg/m³]	1027	1027
Slump [mm]	160 ± 10	145 ± 10
Air content [% volume]	2.8	3.4

Ten concrete specimens per concrete composition were cast in plastic moulds of 150x150x150 mm3 according to [ASTM C192 / C192M]. Specimens fabricated with CEM I and CEM III/B were henceforth named PC and BFS specimens, respectively. After casting, the moulds were wrapped in plastic and kept in laboratory conditions (23 °C, 65% RH) for 24 hours. Subsequently, the specimens were de-moulded and stored in a fog room (23 °C, 95% RH). The cover depth in all concrete specimens was reduced with a water-cooled diamond saw at an age of 7 days old. The post sawing concrete cover in PC specimens was 15mm whereas a reduced cover depth of 10mm was used in the BFS specimens in order to reduce the time to corrosion initiation. The final geometry of PC and BFS specimens is shown in Figure 3. After cutting, the specimens were placed back into the fog room until an age of 28 days old.

2.4 Exposure

Before the specimens were subject to chloride penetration, the mould finished sides of the specimens were coated with an epoxy resin to prevent the ingress of chlorides following the recommendations given in [ASTM C1556/C1556M]. Subsequently, the specimens were exposed to a solution of 3.3% NaCl under laboratory conditions (23 °C, 65% RH). Two
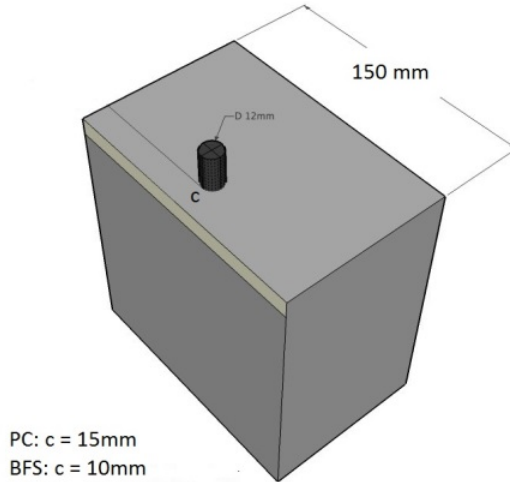
Figure 3. Geometry of reinforced concrete specimens

large plastic containers were used to store the solution and the specimens of each concrete composition. The specimens were partially immersed at a height of 120 mm (Figure 4) at an age of 28 days. A lid prevented evaporation during the experiment. During the duration of the test, no replacement of the solution was performed. For both series of specimens, a saturated calomel electrode (SCE) immersed in the chloride solution was used as a reference electrode for electrochemical measurements.

2.5 *Open circuit potential measurements (OCP)*

Monitoring of the electrochemical potential was performed by immersing a saturated calomel electrode (SCE) in the chloride solution (see below); one SCE for each group of
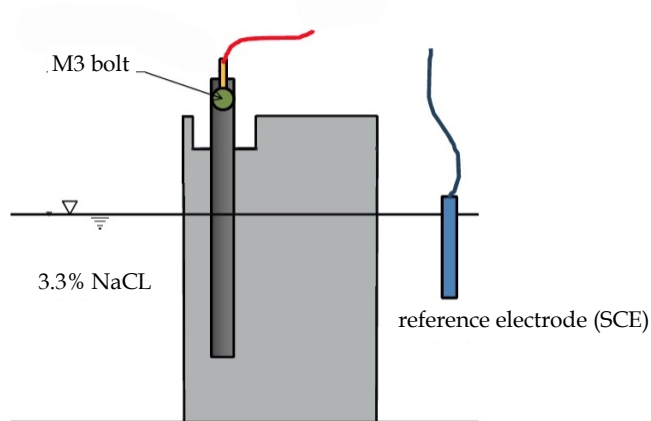

Figure 4. Schematic representation of the exposure and electrochemical measurements
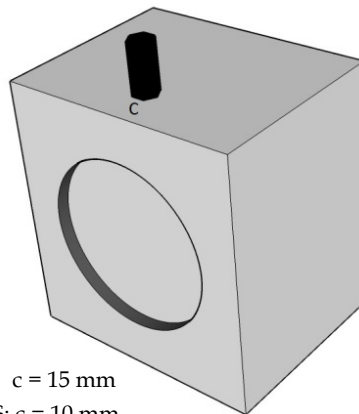
specimens (PC, BFS). A high impedance voltmeter was connected to a multiplexer that allowed continuous measurements of the electrochemical potential of each bar versus SCE (V_{SCE}) reference electrode at intervals of 12 hours.

2.6 *Corrosion initiation*

Initiation of corrosion was considered when a shift in the electrochemical potential of steel towards more negative values fulfilled two conditions: that the shift was at least 100 mV_{SCE} in magnitude; and that the shift persisted for at least 7 days. In case any of these two conditions were not satisfied, the specimen was kept in exposure. When corrosion initiation was confirmed, the specimen was removed from the solution and analysed for chlorides as explained below.

2.7 *Chloride concentration sampling and analysis*

Figure 5 shows a schematic of the sampling applied to the specimens. An area of 80 cm² was ground in layers of 1 mm thick, producing between 8 to 10 grams of powder per layer. During this process, the equipment and the concrete specimen were cleaned with ethanol at the end of each grinding step. The concentration of chlorides by mass of binder was obtained by acid dissolution and subsequent titration according to [ASTM C 1152/1152M]. The ground material was weighed and digested in concentrated nitric acid (1 + 1) followed by fast boiling (10 seconds) and then cooled down to room temperature. Filtering was carried out using a vacuum pump. The filtrate was titrated for chloride. Chlorides were calculated assuming acid dissolved material was cement including (18%) hydration water. Total chloride content was reported as wt. % of cement. Chloride concentrations as

PC: c = 15 mm
BFS: c = 10 mm

Figure 5. Grinding of the concrete cover in concrete specimens

106

a function of depth were fitted to Eq. (1) in order to determine the diffusion coefficient (D_c) and surface content (C_s).

2.8 *Visual examination of steel reinforcement*

After grinding, the embedded steel reinforcement was mechanically extracted from the specimens for visual inspection of the steel surface. Visual observations were focused on the confirmation of the presence of corrosion products at the steel.

3   Results

3.1 *Electrochemical potential measurements*

The electrochemical potential behaviour of steel bars embedded in PC specimens is presented in Figure 6. Results can be divided into three groups with different behaviour: i) a group with a quick potential shift (PC-9 and PC-10); ii) an intermediate group (PC-4 and PC-6); iii) and a long term exposure group (remaining specimens). In all cases, potential shifts of at least -100 mV$_{SCE}$ were observed in all specimens suggesting corrosion initiation. The time necessary for active corrosion to develop for PC-9 and PC-10 were 31 and 34 days, respectively. For the second group it was 82 days (PC-4) and 78 days (PC-6). The
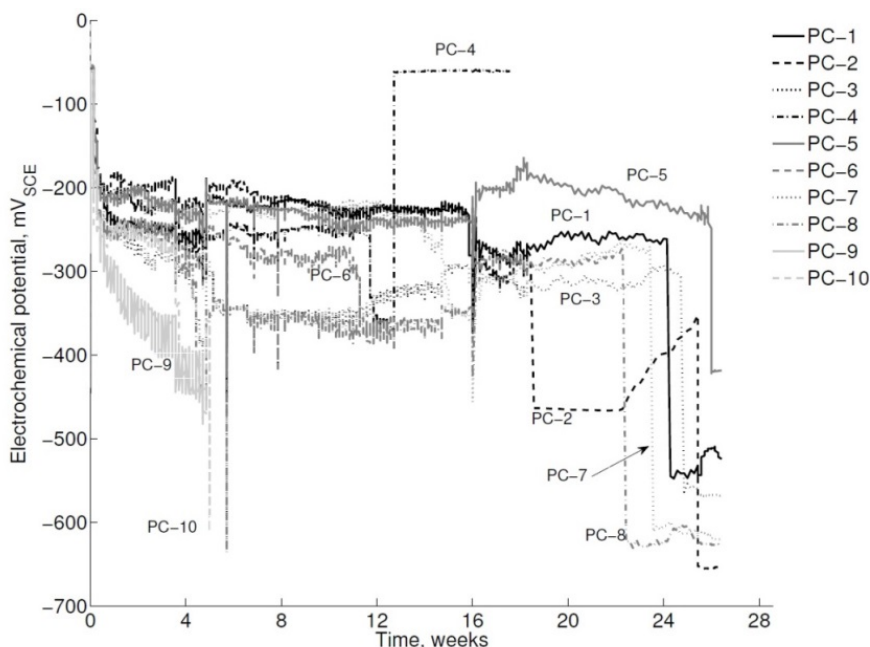
Figure 6. OCP behaviour of PC specimens

final group showed potential shifts at 186 days (PC-1); 195 days (PC-2); 190 days (PC-3); 199 days (PC-5); 179 days (PC-7); and 171 days (PC-8). Also, the shift of OCP towards more negative values remained for at least 7 days, fulfilling the test criteria. Subsequently, specimens were removed from exposure and analysed for chlorides.

Small variations of the electrochemical potential are attributed to changes in the temperature of the room. At the age of 113 days, the temperature and external humidity conditions in the laboratory were not controlled for 72 hours. After the environmental conditions of the room were re-established, the potentials drifted to slightly less noble values for some specimens PC-1, PC-2, PC-3, PC-7 and PC-8. Specimen PC-5's electrochemical potential drifted towards more noble values during this period.

In the case of BFS specimens, as shown in Figure 7, electrochemical potentials of all specimens were located in the region of passivity. These potential values remained stable during the whole exposure period of 28 weeks. This behaviour is significantly different from PC specimens. Based on these results, no sign of reinforcement corrosion is expected from these specimens during the visual inspection (see below).
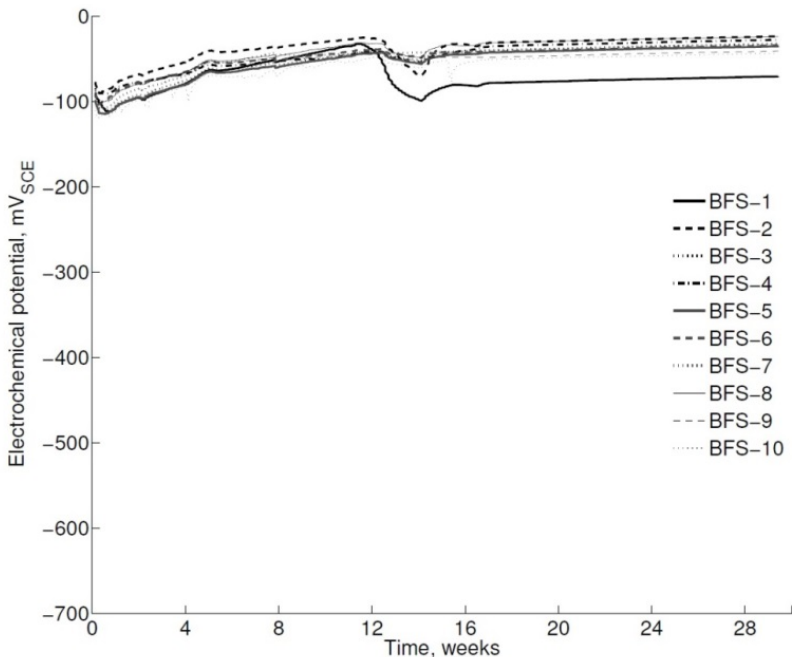

Figure 7. OCP behaviour of BFS specimens

3.2 Chloride concentrations

The chloride contents for all PC specimens in each 1 mm layer of the cover (15 mm) are shown in Table 3. In general, chloride concentrations were between 2.5 and 3.4 wt. % of cement in the first two outer layers of the cover. The chloride concentration at the level of the reinforcement ranged between 0.3 to 1.0 wt. % of cement. The lowest levels were found in specimens PC-9 and PC-10 (0.3 wt. %), the specimens that showed the earliest signs of corrosion. The second group of specimens (PC-4 and PC-6) showed chloride concentrations between 0.4 and 0.6 wt. % of cement. The last group with over 170 days of exposure had values between 0.6 and 1.0 wt. % of cement. At the level of the reinforcement (15 mm) the average chloride concentration of all specimens within this series is 0.56 wt. % of cement with a standard deviation of 0.2 %. These values correspond well with other chloride

Table 3. Chloride concentration (wt. % of cement) and diffusion coefficient (m²/s) in PC specimens, exposed from 28 days age until corrosion initiation

Depth [mm]	PC-1	PC-2	PC-3	PC-4	PC-5	PC-6	PC-7	PC-8	PC-9	PC-10
1 – Surface	3.4	2.9	3.1	2.6	2.5	2.6	2.8	2.6	3.1	3.4
2	3.2	3.3	3	2.9	3.1	2.7	2.9	2.8	2.3	3.4
3	2.0	1.9	2.8	2.4	2.6	2.4	2.5	2.6	1.8	3.3
4	1.6	1.7	2.0	1.8	2.3	2	2.4	1.9	1.5	2.4
5	1.3	1.6	1.8	1.6	1.7	1.7	2.3	1.6	1.6	2.6
6	1.5	1.5	1.5	1.3	1.4	1.5	1.6	1.7	1.7	2.3
7	1.6	1.4	1.4	1.0	1.3	1.4	1.7	1.1	1.4	2.0
8	1.3	1.4	1.3	0.9	1.1	1.3	1.3	0.9	1.3	1.7
9	1.2	1.0	1.1	0.7	1.0	1.0	1.2	0.7	1.2	1.5
10	1.0	1.1	0.9	0.6	0.9	0.9	0.8	0.6	1.2	1.1
11	0.7	0.9	0.8	0.5	0.8	1.1	0.6	0.5	0.9	0.8
12	0.6	0.7	0.7	0.6	0.7	0.7	0.4	0.4	1.1	0.6
13	4.4	0.6	0.8	0.4	0.9	0.6	0.5	0.5	1.0	0.4
14	0.5	0.7	0.6	0.4	0.7	0.5	0.6	0.5	0.8	0.5
15 – Steel	0.6	0.7	0.7	0.4	1.0	0.6	0.5	0.5	0.3	0.3
$t_{corrosion}$ [d]	186	195	190	82	197	78	179	171	31	34
D_c [x 10^{-12} m²/s]	2.4	3.0	2.7	4.3	3.1	7.9	2.7	2.2	27	14.5
C_s [wt. % cement]	3.3	3.0	3.3	3.2	3.0	2.9	3.4	3.2	2.7	4.0
Age [$t_{corrosion}$ + 28 d]	214	223	218	110	225	106	207	199	59	62

threshold data [Breit, 1998, Polder & de Rooij, 2005]. The average C_s obtained from curve fitting was 3.2 wt. % of cement with a standard deviation of 0.3%.

Results presented in Table 3 show that the first group of corroding specimens, PC-9 and PC-10, had the highest diffusion coefficients (D_c): 26.7 x 10^{-12} m²/s and 14.5 x 10^{-12} m²/s, respectively. These values are one order of magnitude higher than those of the rest of the specimens. This could be caused by the increased porosity, compaction defects and defects at the concrete-steel interface that were found after opening the specimens. The Dc of specimens in the second group were 4.37 x 10^{-12} m²/s for PC-4 and 7.93 x 10^{-12} m²/s for PC-6. Finally, the third group of specimens produced lower D_c of 2.43, 3.03, 2.71, 3.13, 2.79 and 2.26 x 10^{-12} m²/s for specimens PC-1, PC-2, PC-3, PC-5, PC-7 and PC-8, respectively. The average D_c (when discarding PC-9 and PC-10) is 3.4 x 10^{-12} m²/s. Figure 8 shows the chloride profiles in PC specimens.
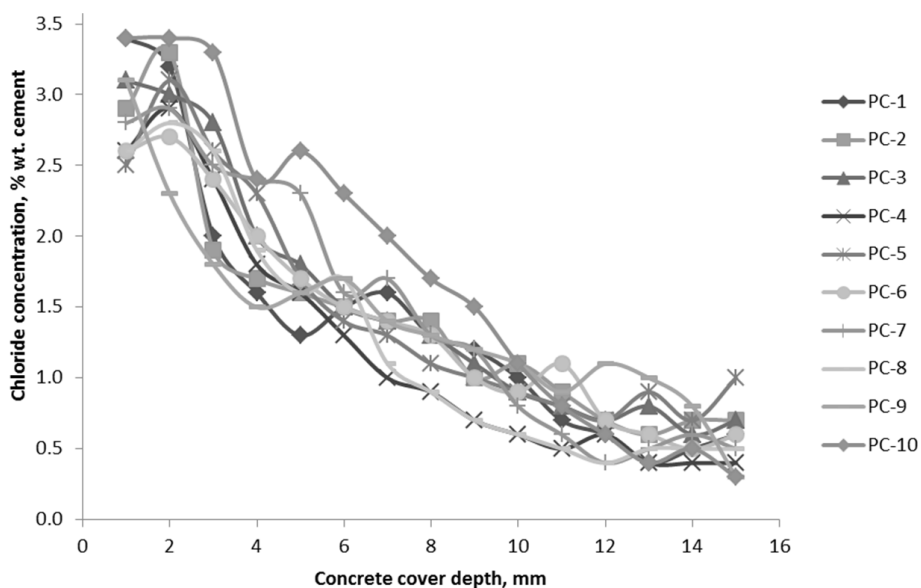

Figure 8. Chloride concentration (wt. % cement) in PC specimens

Regarding BFS specimens, Table 4 shows the result of chloride concentrations at the end of the exposure period of 206 days at different depths (up to 10 mm). Comparing these results with those obtained from the PC specimens, it is clear that the transport of chlorides in BFS

is significantly slower than in PC. At the end of the exposure period, chlorides were not present further than 5 mm from the concrete surface as shown in Figure 9. Average chloride content at the depth of the bar was less than 0.1% with a standard deviation of less than 0.01%. The average D_c in BFS specimens was 1.23 x 10^{-13} m²/s (standard deviation of 0.1 x 10^{-12}) whilst the average C_s obtained from curve fitting was 4.1 % by weight of cement (standard deviation of 0.4%).

Table 4. Chloride concentration (wt. % of cement) and diffusion coefficient (m²/s) in BFS specimens, exposed from 28 to 206 days of age

Depth [mm]	BFS-1	BFS -2	BFS -3	BFS -4	BFS -5	BFS -6	BFS -7	BFS -8	BFS -9	BFS -10
1 – Surface	2.2	2.7	2.5	2.8	2.4	2.5	2.7	2.8	2.9	2.7
2	1.3	1.8	1.4	1.5	1.7	1.6	1.6	1.4	1.5	1.4
3	0.8	0.9	0.8	0.5	0.6	0.4	0.4	0.9	0.3	0.6
4	0.1	0.2	0.3	0.2	0.2	0.1	0.1	0.2	0.1	0.3
5	0.1	0.1	0.1	< 0.1	0.1	< 0.1	0.1	< 0.1	< 0.1	< 0.1
6	< 0.1	< 0.1	< 0.1	< 0.1	< 0.1	< 0.1	< 0.1	< 0.1	< 0.1	< 0.1
7	< 0.1	< 0.1	< 0.1	< 0.1	< 0.1	< 0.1	< 0.1	< 0.1	< 0.1	< 0.1
8	< 0.1	< 0.1	< 0.1	< 0.1	< 0.1	< 0.1	< 0.1	< 0.1	< 0.1	< 0.1
9	< 0.1	< 0.1	< 0.1	< 0.1	< 0.1	< 0.1	< 0.1	< 0.1	< 0.1	< 0.1
10 - Steel	< 0.1	< 0.1	< 0.1	< 0.1	< 0.1	< 0.1	< 0.1	< 0.1	< 0.1	< 0.1
$t_{exposure}$ [d]	206	206	206	206	206	206	206	206	206	206
D_c [x 10^{-13} m²/s]	1.4	1.5	1.4	1.0	1.4	1.1	1.0	1.2	0.8	1.1
C_s [wt. % cement]	3.3	4.3	4.2	3.7	4.6	3.8	4.2	4.5	4.3	4.8
Age [$t_{exposure}$ + 28 d]	234	234	234	234	234	234	234	234	234	234

3.3 *Visual inspection of steel reinforcement*

Figures 10a and 10b show the condition of the steel surface in specimen PC-2 after extraction and the size and location of corrosion pits after cleaning, respectively. These images are representative of the whole series. Pit diameter ranged between approximately 0.5 to 5.0 mm in most cases. This value accounts for the largest diameter of an elliptic geometry. In general, pitting corrosion was observed after 195 days of exposure in all specimens except PC-9 and PC-10. Visual observations of bars from these specimens did not show clear signs of pit formation. However, voids at the concrete-steel interface were found in addition to (bigger) voids in the matrix due to poor compaction of these two specimens.
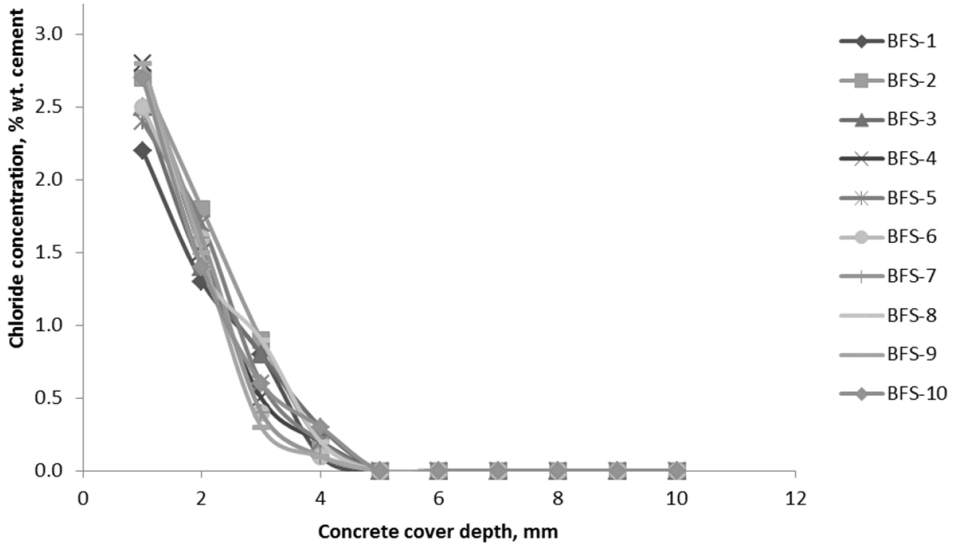
Figure 9. Chloride concentration (wt. % cement) in BFS specimens

a) PC-2 after extraction   b) Corrosion pits in PC-2

Figure 10. Surface condition of steel reinforcement in PC specimens after 6 months of exposure
(Colour figures are available at www.heronjournal.nl .)

Figure 11 shows the surface condition of bars embedded in BFS specimens, with no apparent pitting corrosion. It is confirmed that in the case of BFS specimens, chloride penetration had not reached the depth of the reinforcement at the end of the exposure period.

Figure 11. Surface condition of steel reinforcement in BFS specimens after 6 months of exposure

4   Discussion

4.1   *Electrochemical potentials*

The behaviour of electrochemical potentials of steel bars in PC specimens can be considered as normal compared to the available literature [Angst *et al.*, 2011, Alonso *et al.*, 2000, Alonso *et al.*, 2002]. In some specimens, signs of re-passivation were observed (PC-1 at 15 weeks, PC-5 at 7 weeks) as described by Angst [Angst *et al.*, 2011]

In the case of BFS specimens, no signs of corrosion initiation were observed. Slight variations in the electrochemical potential of steel reinforcement at 15 weeks is attributed to the uncontrolled environmental conditions in the laboratory for a short period of time.

4.2   *Chloride concentrations*

The average corrosion initiating chloride concentrations found in the PC specimens correspond to values found in the literature [François & Arliguie, 1994, Frederiksen, 2009, Polder & de Rooij, 2005]. According to these articles, chloride threshold concentrations for Portland cement concretes have been reported to range between 0.4 and 0.6 wt. % cement. In this study, a mean value of 0.56 wt. % cement was determined, which corresponds well with the range of C_{crit} values. In the case of BFS specimens, chloride concentrations at the

bar depth were lower than 0.1 wt. % of cement. The average fitted values of D_c and C_s for PC specimens were 3.5 x 10^{-12} m²/s and 3.2 wt. % cement, respectively. C_s values obtained in this study correspond well with observed values of C_s in practice [Polder & de Rooij, 2005]. In the case of BFS specimens, the average D_c in BFS concrete was found to be of at least one order of magnitude lower than in PC: 1.3 x 10^{-13} m²/s. The value of C_s fitted in this case was 4.1 wt.% cement. Table 5 shows a summary of results obtained on the two series of specimens.

Table 5. Summary of results of chloride ingress and corrosion initiation in concrete specimens

Series	Cover depth [mm]	C_s [wt. % binder]	D_c [x 10^{-13} m²/s]	Cl at steel level [wt. % cement]	Corrosion initiation
PC	15	3.2	35	0.56	Yes
BFS	10	4.1	1.30	≤ 0.1	No

4.3 *Spatial resolution of the measuring technique*

Research focused on studying C_{crit} is usually carried out by correlating the initiation of corrosion and the chloride content in the cementitious matrix close to the reinforcement meaning that high levels of accuracy are necessary in both aspects of the determination of chloride threshold. Considering the variability of chloride concentrations in concrete, the influence of the scale at which the measuring technique is performed will influence the result.

Generally speaking, there are three working scales in concrete materials research: macro- (cm), meso- (mm) and micro-scale (μm). Another way to describe these working scales is based on the consideration of concrete heterogeneity: homogeneous (macro), bi-phased by accounting aggregates and mortar separately (meso); and multi-phased (micro). Differences obtained from analysis performed on the three working scales may be attributed to the influence of aggregates, porosity, heterogeneity of chloride penetration and limitations of the technique.

4.3.1 Macro scale

Bulk determination of chloride concentrations in ground samples takes into account all chlorides contained in the sample, e.g. the total chloride content. This method requires a relatively large amount of material needed for accurate determination of chloride

concentrations, i.e. 10 g in powder form (c. 4 cm^3 of normal density concrete, 2400 kg/m^3). Results obtained by this method can be questionable when the resolution of the chloride measuring technique (bulk, mm) is larger than the scale on which early pitting corrosion occurs (sub-millimetre) [Angst *et al.*, 2011]. In this sense, the use of quantitative techniques with higher spatial resolution is desirable for determining the concentration of chlorides in the vicinity of sub-millimetre corrosion pits.

4.3.2 Meso scale

Silva [Silva *et al.*, 2011], performed meso-scale localised analysis of the concrete-steel interface in order to determine chloride concentrations associated with localised corrosion initiation. Laser ablation inductively coupled plasma mass spectrometry (LA-ICPMS) measurements were performed by ablating a small volume of concrete, ca. 300 μm in diameter, and analysing the vapour with a mass spectrometer in reinforced specimens subject to chloride penetration. Chloride concentrations were reported based on Cl/CaO ratios. Their study shows semi-quantitatively that the Cl/CaO ratio peaks were found opposite to corrosion pits when analysing the concrete bar imprint. Wilsch *et al.* [32] and Wertiz *et al.* [33]; have studied trace elements and chloride profiles with LIBS (laser induced breakdown spectrometry) in mortar specimens exposed to chloride penetration. Results showed that detecting chlorine was difficult when the concentration was below 6 wt. % cement and later improvements were performed lowering the detection limit to 0.5 wt. % cement. Šavija used the same technique when investigating the ingress of chlorides in cracked concrete [Šavija, 2014]. Results showed that LIBS was able to differentiate between aggregates and mortar (cement + sand) very effectively, while providing quantitative measurements of elements in mortar. Chloride concentration values ranged between 0.1 and 0.8 % of mortar weight. Although this novel technique is still under development, the scale and speed of analysis is promising for investigations on C_{crit} .

4.3.3 Micro scale

On microscopic scale, microanalysis techniques such as Energy Dispersive X-ray Spectrometry (EDS) or Wavelength X-ray Spectrometry (WDS) have been employed for the detection and quantification of elements in concrete [Pacheco & Çopuroğlu, 2015]. Chlorine, and not chloride, is the appropriate term when referring to the concentration of Cl determined by EDS or WDS. Precise chlorine concentrations in samples subject to EDS analysis depend on the appropriate use of reference mineral standards and experimental

parameters [Pacheco & Çopuroğlu, 2015]. Studies by microanalysis techniques reported the Cl signal in either CPS (counts-per-second) or in weight percent of the analysed volume. The analysed volume, ca. 3 μm^3 depending on experimental conditions, allows to study different cement phases such as C-S-H or Afm exclusively which can provide simultaneous information on the concentration of chlorine and other elements in the vicinity of corrosion pits.

5   Summary and Conclusion

This article reports the results obtained from a preliminary version of a proposed method for determining C_{crit} in reinforced concrete. First, reinforced concrete specimens were cast with two different binders: Portland cement (CEM I) and ground granulated blast furnace slag cement (CEM III/B); and with as-received (partially lightly rusted) corrugated reinforcing steel bars. The specimens were subsequently exposed to chloride penetration in 3.3% NaCl solution. Monitoring of the electrochemical potential of embedded reinforcement was used to indicate if corrosion initiation took place; its criterion was when a substantial shift (>100 mV) in the potential towards less noble values was observed for at least 7 days. At the end of the exposure period (6 months), corrosion had initiated in all PC specimens; while in the case of the BFS series, no corrosion occurred, i.e. C_{crit} was not reached. Both cases were confirmed by visual observation of the steel after opening the specimens. Average C_{crit} at the level of the reinforcement was 0.56 wt. % cement for PC specimens. In the case of BFS specimens, the chloride concentration at the level of the reinforcement was ≤ 0.1 wt. % of cement. Both C_{crit} , C_s and D_c in PC specimens found during this test corresponded well to those reported in the literature.

The main conclusions derived from this study are:

- The test method achieved its goal of determining C_{crit} for PC concrete specimens within six months. The duration of the test was not long enough to reach C_{crit} in BFS specimens.
- Even with a reduced concrete cover, BFS concrete specimens outperformed their PC counterparts in the time necessary to reach C_{crit} and with lower concentration of chlorides in the intermediate concrete layers.
- Accurate determination of C_{crit} is strongly dependent on the measuring technique. So far, acid digestion and wet chemical analysis of macroscopic

samples is commonly performed for determining the concentration of chlorides in concrete. This bulk technique, however, lacks the spatial resolution to determine chloride concentrations next to corrosion pits. Meso- and microscale techniques may be more suitable for determining C_{crit} at a spatial scale similar to the scale involved in initiation of corrosion pits.

Literature

Alonso, C., Andrade, C., Castellote, M., & Castro, P. (2000). Chloride threshold values to depassivate reinforcing bars embedded in a standardized OPC mortar. *Cement and Concrete Research*, **30** (7), 1047-1055.

Alonso, C., Castellote, M., & Andrade, C. (2002). Chloride threshold dependence of pitting potential of reinforcements. *Electrochimica Acta*, **47** (21), 3469-3481.

Angst, U., Elsener, B., Larsen, C. K., & Vennesland, Ø. (2009). Critical chloride content in reinforced concrete—a review. *Cement and Concrete Research*, **39** (12), 1122-1138.

Angst, U. M., Elsener, B., Larsen, C. K., & Vennesland, Ø. (2011). Chloride induced reinforcement corrosion: electrochemical monitoring of initiation stage and chloride threshold values. *Corrosion Science*, **53** (4), 1451-1464.

Angst, U. M., & Polder, R.B. (2014). Spatial variability of chloride in concrete within homogeneously exposed areas. *Cement and Concrete Research*, **56**, 40-51.

ASTM C143/C143M. (2004). Standard Test Method for Slump of Hydraulic Cement Concrete.

ASTM C192/C192M. (2007). Standard Practice for Making and Curing Concrete Test Specimens in the Laboratory.

ASTM C231/C231M. (2014). Standard Test Method for Air Content of Freshly Mixed Concrete by the Pressure Method.

ASTM C 1152/1152M. (2003). Standard Test Method for Acid-Soluble Chloride in Mortar and Concrete.

ASTM C1556/1556M (2011). Standard Test Method for Determining the Apparent Chloride Diffusion Coefficient of Cementitious Mixtures by Bulk Diffusion.

Breit, W. (1998). Critical chloride content-Investigations of steel in alkaline chloride solutions. *Materials and Corrosion*, **49** (8), 539-550.

Collepardi, M., Marcialis, A., & Turriziani, R. (1972). Penetration of chloride ions into cement pastes and concretes. *Journal of the American Ceramic Society*, **55** (10), 534-535.

DuraCrete (2000). DuraCrete - General Guidelines for Durability Design and Redesign, *The European Union* - Brite EuRam III BE95-1347/R17.

fib (2006). *Model Code for Service Life Design*, Bulletin 34.

François, R., & Arliguie, G. (1994). Durabilité du béton armé soumis à l'action des chlorures. In *Annales de l'Institut Technique du Batiment et des Travaux Publics* (No. 529 (B-316)).

Frederiksen, J. M. (2009). On the need for more precise threshold values for chloride initiated corrosion. *Materials and corrosion*, **60** (8), 597-601.

Pacheco, J. (2015). *Corrosion of steel in cracked concrete: chloride microanalysis and service life predictions*. PhD Thesis, Delft University of Technology.

Pacheco, J., & Çopuroğlu, O. (2015). Quantitative Energy-Dispersive X-Ray Microanalysis of Chlorine in Cement Paste. Journal of Materials in Civil Engineering, 04015065.

Page, C. L., & Treadaway, K. W. J. (1982). Aspects of the electrochemistry of steel in concrete. *Nature* **297**, 109 – 115.

Polder, R. B., & De Rooij, M. R. (2005). Durability of marine concrete structures: field investigations and modelling. *HERON*, 50 (3).

RILEM TC 235-CTC, Corrosion initiating chloride threshold concentrations in concrete – Test method for determining C_{crit} in laboratory conditions. RILEM, to be published.

Silva, N., Luping, T., & Rauch, S. (2013). Application of LA-ICP-MS for meso-scale chloride profiling in concrete. *Materials and Structures*, **46** (8), 1369-1381.

Šavija, B., Schlangen, E., Pacheco, J., Millar, S., Eichler, T., & Wilsch, G. (2014). Chloride ingress in cracked concrete: a laser induced breakdown spectroscopy (LIBS) study. *Journal of Advanced Concrete Technology*, **12** (10), 425-442.

Tuutti, K. (1982). *Corrosion of steel in concrete*. Swedish Cement and Concrete Research Institute. Stockholm.

Weritz, F., Schaurich, D., & Wilsch, G. (2007). Detector comparison for sulfur and chlorine detection with laser induced breakdown spectroscopy in the near-infrared-region. *Spectrochimica Acta Part B: Atomic Spectroscopy*, **62** (12), 1504-1511.

Wilsch, G., Weritz, F., Schaurich, D., & Wiggenhauser, H. (2005). Determination of chloride content in concrete structures with laser-induced breakdown spectroscopy. *Construction and Building Materials*, **19** (10), 724-730.